

Polytypism, homochirality, interpenetration, and hydrogen-bonding in transition metal (Mn(II), Ni(II), Cu(II), Zn(II)) 5-hydroxyisophthalate coordination polymers containing 4,4'-bipyridyl†‡

Russell K. Feller and Anthony K. Cheetham*

Received 31st October 2007, Accepted 8th January 2008

First published as an Advance Article on the web 19th February 2008

DOI: 10.1039/b716454h

We report the synthesis of five coordination polymers of divalent transition metals combined with 5-hydroxyisophthalic acid (HIP) and 4,4'-bipyridyl (bipy). Mn forms two polytypic two-dimensional coordination polymers, Mn(HIP)(bipy)·3H₂O and Mn(HIP)(bipy)· $\frac{1}{4}$ bipy·2H₂O (**I** and **II**, with ABAB and ABC stacking sequences, respectively); Ni forms a chiral hexagonal three-dimensional coordination polymer with two interpenetrating trigonal sublattices exhibiting the “dual quartz” topology, Ni(HIP)(bipy)(H₂O) (**III**); Cu forms a one-dimensional coordination polymer containing arrays of infinite hydrogen-bonded molecular ribbons, Cu(HIP)₂(bipy) (**IV**); and Zn forms a two-dimensional coordination polymer with a stair-stepped layered structure, Zn₂(HIP)₂(bipy)(H₂O)₂·H₂O (**V**). The M–HIP–M connections are perpendicular to the M–bipy–M connections in all structures where they are present.

Introduction

Hybrid inorganic–organic framework structures have attracted widespread attention in recent years. Since 1990, many compounds of this type have been discovered which also incorporate polyfunctional organic molecules as key structural elements, bridging the metal centers *via* covalent bonds.¹ The majority of these compounds are prepared through mild hydrothermal or solvothermal syntheses, at temperatures below 200 °C. The flourishing diversity of structures and dimensionalities seen in these coordination polymers has caused them to grow into a major field of research.²

5-Hydroxyisophthalic acid has proven to be an effective connecting ligand in the construction of coordination polymers. It is known to form such compounds with alkaline earths,³ transition metals⁴ and lanthanides.⁵ These structures often contain kinked chain motifs due to the molecule's bent rod-like geometry. By incorporating capping ligands such as 2,2'-bipyridyl, 2-(pyrazol-3-yl)pyridine or 1,10-phenanthroline to restrict connectivity in such systems,^{4a,6} or rigid linkers such as 4,4'-bipyridyl or 1,2-bis(4-pyridyl)ethene to increase connectivity,⁷ compounds with many different framework topologies have been prepared. In the present work, coordination polymers containing divalent Mn, Ni, Cu or Zn combined with 5-hydroxyisophthalate (HIP) and 4,4'-bipyridyl (bipy), were synthesized with differing stoichiometries and ionization states of 5-hydroxyisophthalic acid. Subtle differences in the preferred coordination geometries of these four metals have led to

markedly different structures in the corresponding coordination polymers.

Experimental

Materials

All reagents were used as purchased; Mn(OAc)₂·4H₂O (99+%), Zn(OAc)₂·2H₂O (98+%), Ni(OAc)₂·4H₂O (98%), Cu(OAc)₂·H₂O (98+%) and 5-hydroxyisophthalic acid (97%) from Aldrich, and 4,4'-bipyridyl (98%) from Alfa Aesar. Syntheses were carried out in 23 mL Parr Teflon-lined stainless-steel autoclaves under autogenous pressure. Elemental analysis (C, H, N) was carried out by the Marine Sciences Institute Analytical Laboratory at UCSB.

Synthesis of **I** and **II**

Yellow blocks of Mn(HIP)(bipy)·3H₂O (**I**) were obtained by heating a mixture of 1 mmol Mn(OAc)₂·4H₂O, 1 mmol 5-hydroxyisophthalic acid, 0.5 mmol 4,4'-bipyridyl and 5 mL deionized water for 2 days at 180 °C. The product was cooled to room temperature, vacuum-filtered and rinsed with deionized water. Yellow blocks of Mn(HIP)(bipy)· $\frac{1}{4}$ bipy·2H₂O (**II**) were obtained similarly, but using 1 mmol 4,4'-bipyridyl in the mixture. Higher concentrations of 4,4'-bipyridyl in the reaction mixture favor the crystallization of **II** over **I** because **II** can accept guest 4,4'-bipyridine molecules. Phase-pure samples of **I** could not be obtained, so CHN analysis was not performed on this material. Subsequently, a phase-pure powder of **II**, as confirmed by powder X-ray diffraction, was obtained in ~90% yield by using an excess (1.5 mmol) of 4,4'-bipyridyl, and additionally rinsing with acetone. CHN analysis of this powder suggests that the bipy content of the bulk powder used for the analysis may be slightly greater than that in the single crystal, in agreement with the difference in synthesis conditions. Found (wt%): C, 56.01%; H, 3.50%; N, 8.02%. Calc'd (wt%): C, 52.80%; H, 3.90%; N, 7.51%.

Materials Research Laboratory, University of California, Santa Barbara, CA 93106-5121, USA. E-mail: cheetham@mrl.ucsb.edu

† CCDC reference numbers 657326–657330. For crystallographic data in CIF or other electronic format see DOI: 10.1039/b716454h

‡ Electronic supplementary information (ESI) available: Tables of bond lengths and angles, anisotropic displacement parameters, hydrogen coordinates and hydrogen bond parameters; and powder diffractograms and thermal analysis for **II**, **IV** and **V**. See DOI: 10.1039/b716454h

Synthesis of III

Bright blue hexagonal pyramids of Ni(HIP)(bipy)(H₂O) were obtained by heating a mixture of 1 mmol Ni(OAc)₂·4H₂O, 1 mmol 5-hydroxyisophthalic acid, 0.5 mmol 4,4'-bipyridyl and 5 mL deionized water for 2 days at 200 °C. The product was cooled to room temperature, vacuum-filtered and rinsed with deionized water. A yield of several isolated crystals (<5% of the solid product) was obtained. A slightly better yield (~10% of the solid) of polycrystalline clusters was obtained at 220 °C using either 0.5 mmol or 1 mmol 4,4'-bipy, but **III** still remained a minority phase. No crystals of the light blue majority phase large enough for structure determination were obtained, and its powder diffraction pattern could not be matched. Elemental analysis and a powder diffractogram of **III** are not available as a phase pure sample was not synthesized.

Synthesis of IV

Deep purple plates of Cu(HIP)₂(bipy) were obtained by heating a mixture of 1 mmol Cu(OAc)₂·H₂O, 1 mmol 5-hydroxyisophthalic acid, 1 mmol 4,4'-bipyridyl and 5 mL deionized water for 2 days at 150 °C. The product was cooled to room temperature, vacuum-filtered and rinsed with deionized water. Subsequently a phase-pure powder, as confirmed by powder X-ray diffraction, was obtained in ~90% yield by heating 0.75 mmol Cu(OAc)₂·H₂O, 1.5 mmol 5-hydroxyisophthalic acid, 0.75 mmol 4,4'-bipyridyl and 5 mL deionized water at 125 °C, and additionally rinsing with acetone. Found (wt%): C, 53.04%; H, 3.05%; N, 4.59%. Calc'd (wt%): C, 53.65%; H, 3.12%; N, 4.81%.

Synthesis of V

Pale tan blocks of Zn₂(HIP)₂(bipy)(H₂O)₂·H₂O were obtained in ~90% yield by heating a mixture of 1 mmol Zn(OAc)₂·2H₂O, 1 mmol 5-hydroxyisophthalic acid, 0.5 mmol 4,4'-bipyridyl and 5 mL deionized water for 2 days at 200 °C. The product was cooled to room temperature, vacuum-filtered and rinsed with deionized water and then acetone. Powder X-ray diffraction confirmed that the product is phase-pure under these conditions, and remains so when treated at temperatures as low as 125 °C. Found (wt%): C, 44.30%; H, 2.99%; N, 3.73%. Calc'd (wt%): C, 44.53%; H, 3.17%; N, 4.00%.

Structure determinations†

Suitable single crystals were selected under a polarizing microscope and glued to glass fibers. Intensity data were collected at room temperature on a Siemens SMART CCD diffractometer (Mo K α radiation, $\lambda = 0.71073$ Å). The structures were solved using direct methods and difference Fourier synthesis, and refined against $|F|^2$ using the *SHELXTL* software package.⁸ **IV** was initially solved in the *Cc* space group and **V** was initially solved in the *P1* space group, and both structures were subsequently transformed into the corresponding centrosymmetric space groups using the *PLATON* software package.⁹ Psi-scan absorption corrections for **I** and **II** were made using the *XPREP* module of *SHELXTL*, and multi-scan absorption corrections for **III–V** were made using *SADABS*.¹⁰ The extinction coefficients all

refined to within three E.S.D.'s of zero, and were thus removed from the refinements. All non-hydrogen atoms were refined anisotropically. The Flack parameter for **III** was $-0.05(2)$.¹¹ CCDC deposition numbers: 657326 for **I**, 657327 for **II**, 657328 for **III**, 657329 for **IV**, and 657330 for **V**. See Table 1 for crystal data and structure refinement parameters.

In **I** and **II**, riding hydrogens were added to the phenyl carbons, and water hydrogens were not located due to disorder, as described below. One of the two rings of the uncoordinated bipy molecule in **II** was restrained to planarity, with the other ring being crystallographically equivalent. An anti-bumping restraint was placed on its central C–C bond, with other bond distances restrained to be similar to those in the coordinated bipy molecule. C25, OW2 and OW4 were lightly restrained to approximate isotropic behavior. In **III**, riding hydrogens were added to the phenyl carbons but the water and phenol hydrogen positions were refined, with all three O–H distances restrained to be similar and one thermal parameter used for both water hydrogens. In **IV**, riding hydrogens were added to the phenyl carbons, but the phenol and carboxyl hydrogens were freely refined. In **V**, all hydrogen atom positions were refined, with some C–H and O–H distances restrained to chemically reasonable values. One thermal parameter was refined for each set of chemically equivalent hydrogens, with those of the coordinated water molecule differentiated from those of the uncoordinated water molecule. Atoms of the uncoordinated water molecule were given occupancy factors of 1/2, as this molecule appears disordered across an inversion center, as described below.

The presence of domains of **I** within **II** and *vice versa* due to stacking faults, along with severe disorder in the guest water molecules, complicated the structural solutions and refinements somewhat, with **II** being more affected. Intensity data collected at 120 K offered no improvement in the final refinement statistics nor in the location of the disordered water. In addition, because crystal mosaicity appeared to have increased after cooling, the room temperature data were used. It was found that refinement statistics were improved by performing psi-scan absorption corrections rather than multi-scan corrections.

Thermal analysis

TGA/DTA analysis of **II**, **IV** and **V** was performed in air on a Mettler 851e TG/sDTA up to 600 °C. Temperatures were ramped at 5 °C min⁻¹. For **II**, a gradual mass loss of 3.1% (7.7% expected for loss of guest water, or 8.4% for loss of guest bipy), occurred between 100–200 °C, accompanied by a very slight endotherm in the DTA trace. Between 200–400 °C, but mostly after 300 °C, a further mass loss of 80.0% occurred, with a large corresponding exotherm in the DTA beginning at 350 °C. After both events, 16.9% of the original mass remained (15.2% expected for complete transformation to MnO, or 16.4% for Mn₃O₄). For **IV**, a single sharp mass loss of 84.7% occurred between 275–350 °C, with a sharp corresponding exotherm in the DTA beginning at 310 °C. After this event, 15.3% of the original mass remained (13.7% expected for complete transformation to CuO). It was found that **IV** expands significantly during decomposition, which limited the sample size that could be safely used in the instrument. Accordingly, the apparent mass gain due to sample buoyancy (~1.4%) was taken into account in calculating the

Table 1 Crystal data and structure refinement parameters

Compound	I	II	III	IV	V
Abbreviated formula	Mn(HIP)(bipy)·3H ₂ O	Mn(HIP)(bipy)· $\frac{1}{4}$ bipy·2H ₂ O	Ni(HIP)(bipy)(H ₂ O)	Cu(HIP) ₂ (bipy)	Zn ₂ (HIP) ₂ (bipy)-(H ₂ O) ₂ ·H ₂ O
Formula weight	445.28	466.31	413.02	581.96	701.20
<i>T</i> /K	298(2)	298(2)	298(2)	298(2)	298(2)
Crystal system	Monoclinic	Monoclinic	Hexagonal	Monoclinic	Triclinic
Space group	<i>P</i> 2/ <i>c</i>	<i>P</i> 2/ <i>n</i>	<i>P</i> 6 ₁	<i>C</i> 2/ <i>c</i>	\bar{P}
<i>a</i> /Å	10.1726(11)	11.6900(8)	11.2217(7)	10.118(3)	7.4720(14)
<i>b</i> /Å	11.6397(13)	10.1772(7)	11.2217(7)	11.051(3)	9.6175(18)
<i>c</i> /Å	16.2535(18)	17.9098(12)	25.0290(16)	21.051(5)	10.1060(19)
<i>a</i> /°	90	90	90	90	100.587(3)
<i>β</i> /°	103.310(3)	102.326(2)	90	99.029(5)	97.165(3)
<i>γ</i> /°	90	90	120	90	112.381(3)
<i>V</i> /Å ³	1872.8(4)	2081.6(2)	2729.6(3)	2324.5(10)	644.8(2)
<i>Z</i>	4	4	6	4	1
ρ_{calc} /g cm ⁻³	1.579	1.488	1.508	1.663	1.806
μ /mm ⁻¹	0.756	0.681	1.103	1.007	1.938
<i>F</i> ₀₀₀	916	958	1272	1188	356
Crystal size/mm	0.20 × 0.18 × 0.15	0.18 × 0.15 × 0.12	0.25 × 0.15 × 0.15	0.30 × 0.10 × 0.03	0.40 × 0.30 × 0.20
θ range/°	2.06 to 26.91	2.00 to 26.73	2.10 to 27.68	1.96 to 26.73	2.37 to 26.02
Refls collected	15276	16826	15724	9477	5163
Ind. reflections	3893	4239	3553	2346	2485
<i>R</i> _{int}	0.0971	0.0472	0.0433	0.0533	0.0238
Completeness (%)	96.0	95.7	94.8	95.7	97.5
Abs. correction	Psi-scan	Psi-scan	SADABS	SADABS	SADABS
# of parameters	320	327	257	187	240
G.O.F. on <i>F</i> ²	0.929	1.071	1.055	1.048	1.065
<i>R</i> ₁ , <i>wR</i> ₂ [for all <i>I</i> > 2σ(<i>I</i>)]	0.0581, 0.1313	0.0728, 0.2284	0.0497, 0.1137	0.0525, 0.1152	0.0439, 0.1041
<i>R</i> ₁ , <i>wR</i> ₂ [for all reflections]	0.1083, 0.1486	0.1040, 0.2428	0.0608, 0.1193	0.0851, 0.1316	0.0560, 0.1119
Largest diff. peak and hole/e Å ⁻³	0.698, -0.325	1.234, -0.616	1.375, -0.306	0.877, -0.300	0.703, -0.321

percentages above, but was negligible for **II** and **V**. For **V**, a mass loss of 7.2% (7.7% expected for loss of all water), occurred between 75–175 °C, accompanied by a small endotherm in the DTA trace. Between 375–450 °C, a further mass loss of 68.4% occurred, with a large corresponding exotherm in the DTA beginning at 410 °C. After both events, 24.2% of the original mass remained (23.2% expected for complete transformation to ZnO). See ESI† for full data.

Results and discussion

Structures of **I**, Mn(HIP)(bipy)·3H₂O, and **II**, Mn(HIP)(bipy)· $\frac{1}{4}$ bipy·2H₂O

Compound **I** (Fig. 1) crystallizes in the space group *P*2/*c*, and **II** (Fig. 2) crystallizes in *P*2/*n*. Both are two-dimensional coordination polymers containing the same layer motif (Fig. 3), with layers lying in (002) planes, but the layer-inversion patterns and the directions and sequences of stack-slipping differ. Layers consist of dimers of distorted *trans*-MnN₂O₄ octahedra, which form eight-membered M–OCO–M–OCO rings. These dimers are connected in one direction by pairs of HIP ligands, and in another by bipy ligands. Similar layers are seen in Mn–bipy–isophthalate and Cd–bipy–isophthalate frameworks which have also been reported in *P*2/*c* with nearly identical cell parameters.¹² Each octahedron has one pair of oxygens splayed apart (O–Mn–O

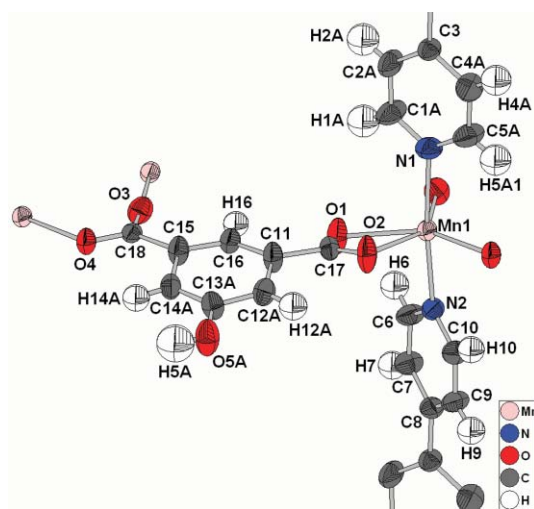


Fig. 1 Thermal ellipsoid plot (50% probability) of **I**, with the atoms of one asymmetric unit labeled. Disordered water molecules and minority (“B”) disorder components are omitted for clarity.

angle 124.7(1)° in **I**), and the opposite pair pinched together (O–Mn–O angle 56.4(1)° in **I**). The pairs of HIP ligands are oriented in such a way as to create two symmetry-equivalent C–H...O close contacts (*d*(C...O) = 3.508(4) Å in **I**, C–H...O angle = 169.8(2)° in **I**), possibly indicative of Ar–H...O hydrogen bonding. Similar

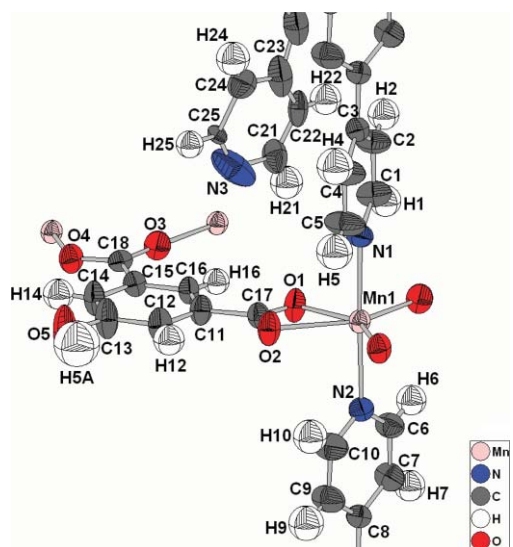


Fig. 2 Thermal ellipsoid plot (50% probability) of **II**, with the atoms of one asymmetric unit labeled. Disordered water molecules are omitted for clarity.

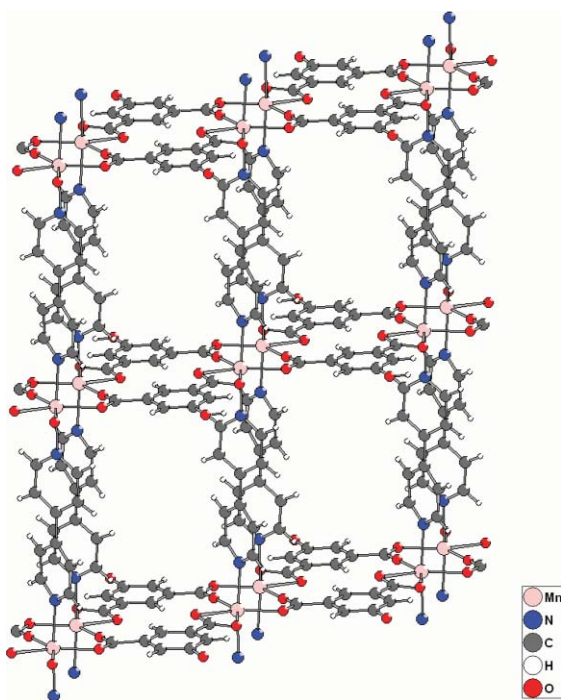


Fig. 3 A portion of one Mn(HIP)(bipy) layer as found in **I** and **II**. Pairs of Mn^{2+} cations are bridged by pairs of HIP ligands in one direction, and by pairs of bipy ligands in another.

pairs of HIP ligands are seen in several of the other structures previously referred to.^{4d,6}

Compound **I** exhibits ABAB stacking (Fig. 4), with layers alternatingly shifted $\pm 1/6$ along b and with stack-slipping along a . Compound **II** exhibits a pseudo-ABC stacking (Fig. 5), with a shift of nearly $1/3$ per layer along a due to stack-slipping, and 180° rotation of every other layer. In **I**, the stacking slips parallel to the M–HIP–M connections, but in **II** the stacking slips parallel to the M–bipy–M connections. The interlayer distances are 7.91 \AA

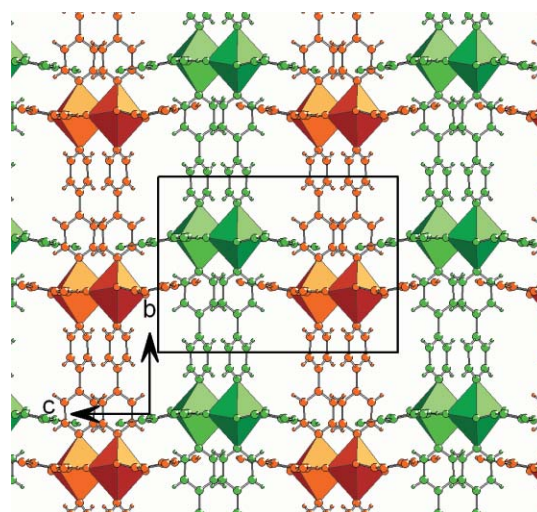


Fig. 4 ABAB-type stacking of layers in **I**, viewed from the side, with layers colored orange or green according to the stacking sequence. Extra-framework molecules are omitted for clarity.

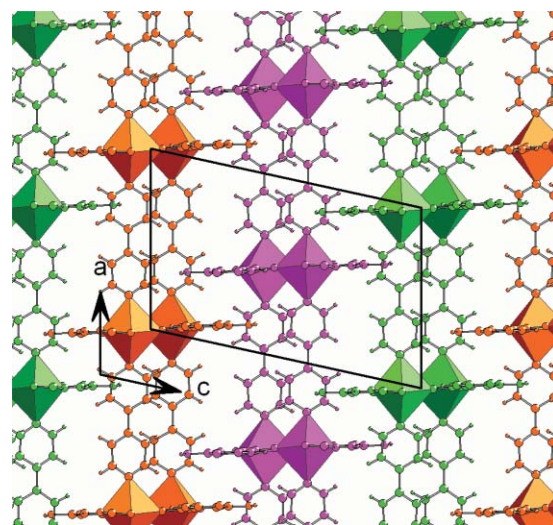


Fig. 5 ABC-type stacking of layers in **II**, viewed from the side and to the same scale as in Fig. 4, with layers colored orange, purple or green according to the stacking sequence. Extra-framework molecules are omitted for clarity.

in **I**, and 8.75 \AA in **II**, and the densities differ correspondingly: 1.579 g cm^{-3} and 1.488 g cm^{-3} , respectively.

Both **I** and **II** contain disordered uncoordinated water molecules, which could be located at several sites between the layers, whose occupancies were all fixed at $1/2$, and some of which are in positions that suggest interlayer hydrogen bonding. Water in **I** occupies $2 \times 5 \text{ \AA}$ channels running along c , and water in **II** occupies $4 \times 3 \text{ \AA}$ channels running along $[101]$. In both compounds, these channels are defined by the rectangular gaps belonging to consecutive layers; they run perpendicular to the layers in **I**, but are obliquely oriented in **II** due to its different stacking sequence. The channels in **II** also host an uncoordinated bipy molecule whose site occupancy was similarly fixed at $1/2$; it shares the space with the water molecules. The uncoordinated bipy molecules stack between the coordinated bipy groups as seen

in He and coworkers' cobalt–bipy–HIP,^{7a} but with the long axis rotated approximately 20° rather than 80°.

In **I**, the HIP ligands are disordered between upward and downward positions, across planes perpendicular to *b*. The occupancy factors for the disordered components are approximately 1/3 and 2/3. The amplitude of the disorder appears much smaller in **II**, and was not resolvable into two components. This difference may be because pairs of HIP groups from consecutive layers are much farther apart in **II** (3.4 Å face-to-face) than in **I** (2.9 Å), where they experience stronger van der Waals interactions. Additionally, one ring of every bipy ligand in **I** is torsionally disordered between two positions differing by 44° in rotation, because there are no neighboring moieties to confine it. In **II**, both rings of the bipy ligands are confined by other groups, so no torsional disorder is present. Similar reported structures to **I** and **II**, such as the aforementioned bipy–isophthalates, show analogous types of disorder. Tao and coworkers' Cd–bipy–isophthalate^{12b} shows significant up/down disorder in its isophthalate rings, but little disorder of the bipy ligands, whereas Ma and coworkers' Mn–bipy–isophthalate^{12a} is reported with all the isophthalate rings in one position, but the thermal ellipsoids suggest unresolved torsional disorder of one ring of the bipy ligands, as in **I**. Both of these compounds have stacking patterns analogous to **I**, and neither exhibits the 180° rotation of alternating layers seen in **II**.

Polytypism between coordination polymers has been referred to previously, with different examples deviating by varying extents from the strictest definition of the phenomenon. β-CuNCS, which might be considered an extremely simple coordination polymer, has been reported by Smith and Saunders to exhibit ABAB and ABC polytypes reminiscent of wurtzite and sphalerite.¹³ Polytypism has been claimed between the chain-like compounds diethylammonium lead(II) iodide and alaninium tin(II) iodide,¹⁴ but in addition to their largely differing chemical constituents, these two compounds differ both in their intra-chain topology and in their chain packing arrangement. However, multiple packings of the same chain motif, which might be considered a form of “rod polytypism”,¹⁵ occur both in Groves and coworkers' lanthanum bis(phosphonomethyl)piperazinium chlorides¹⁶ as well as Kurmoo and coworkers' and Chen and coworkers' nickel 1,4-cyclohexanedicarboxylates.¹⁷ While **I** and **II** in the present work differ partially in their guest molecules, they are the truest example of polytypism among coordination polymers in that their principal structural difference is in the stacking of the same layer motif.

Structure of **III**, Ni(HIP)(bipy)(H₂O)

Compound **III** (Fig. 6) crystallizes in the space group *P*6₁ and is a three-dimensional chiral coordination polymer consisting of two interpenetrating sublattices with only weak interactions between them. Nickel cations sit in *trans*-NiN₂O₄ octahedra with one short (2.000(3) Å) and one long (2.181(3) Å) Ni–O bond, and the long bond is bent approximately 25° out of perpendicularity to its neighbors. The *trans* coordination of the bipy ligands generates layers of parallel Ni–bipy chains (Fig. 7) which lie in (006) planes, while the HIP ligands connect these layers perpendicularly, winding about the *c* direction. (A copper–bipy–succinate in *P*6₁ has been reported by Zheng and Kong to contain similar sheets connected by succinate anions along the *c* direction, but all layers are covalently connected.¹⁸) Each nickel is coordinated

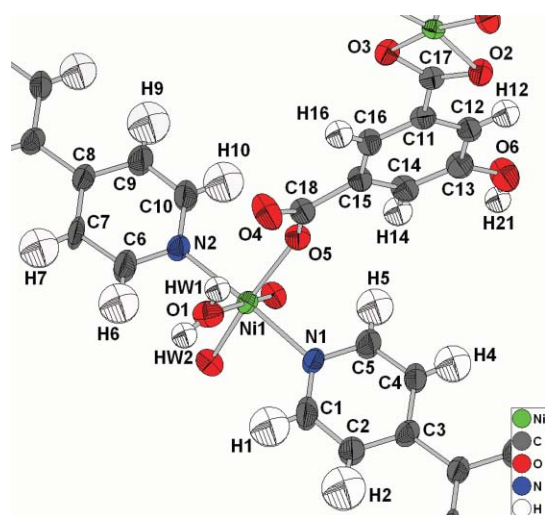


Fig. 6 Thermal ellipsoid plot (50% probability) of **III**, with the atoms of one asymmetric unit labeled.

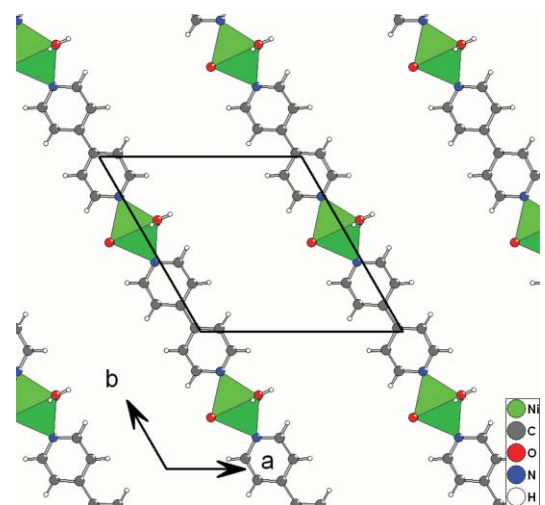


Fig. 7 One layer of nickel–bipy chains in **III**, lying in a (006) plane.

from below (*−c*) by both oxygens of one HIP carboxyl group, and from above (*+c*) by one oxygen of the other carboxyl group of a different HIP ligand, with one aqua ligand occupying the remaining coordination site above. Alternating layers of the Ni–bipy chains are covalently connected by HIP ligands, with no bonding between consecutive layers, hence two sublattices are formed (Fig. 8). Within one sublattice, consecutive layers are rotated 120°, with three layers per cell, and thus each sublattice possesses 3₁ symmetry. The collinearity of the two 3₁ axes and the equal spacing of contributions from the two sublattices give rise to the overall 6₁ symmetry. The aqua ligand donates an intralattice hydrogen bond to the non-coordinating carboxyl oxygen, as well as an interlattice hydrogen bond to one of the coordinating carboxyl oxygens on the nickel cation one layer above (Fig. 9). Additionally, the phenol group donates an interlattice hydrogen bond to the non-coordinating carboxyl oxygen belonging to the nickel cation one layer below. The projection of the Ni–HIP helices alone onto the *ab* plane creates a Kagome-type lattice, with 6 trigonal helices surrounding each hexagonal gap in the lattice (Fig. 10). The bipy

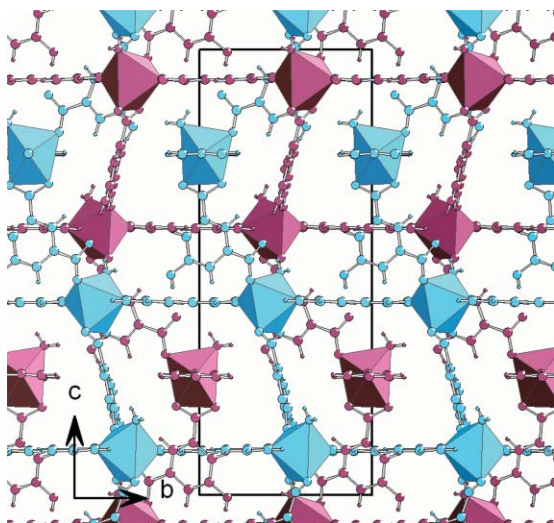


Fig. 8 Packing diagram of **III**, with atoms color-coded by sublattice of origin. Alternating layers of nickel–bipy chains belong to alternating sublattices, with HIP ligands from each sublattice inserting through gaps in the other.

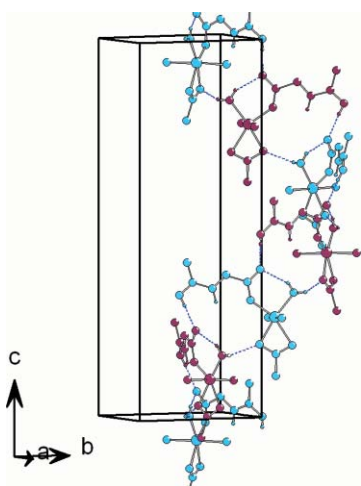


Fig. 9 Helical hydrogen bonding in **III** connecting nickel centers from alternating sublattices, with atoms color-coded by sublattice and hydrogen bonds dotted in dark blue.

ligands are stacked directly on the 6_1 axes, and these stacks occupy the gaps in the Kagome lattice.

While the particular crystal used in our structure determination is chiral, with no indication of racemic twinning, we expect that the sample overall is a conglomerate, with half of the crystals having grown in the opposite-handed space group $P6_5$. Each crystal's chirality is imparted not by any of the individual components, which are all achiral, but by the helical arrangement of these components.

The Schläfli vertex symbol for each sublattice of **III** was determined using the TOPOS software package¹⁹ to be $(7^5;9)$, corresponding to the dense “dual quartz” topology, with each nickel center connecting to four nearest neighbors in a distorted see-saw geometry. Carlucci *et al.* have reported a triply-interpenetrating framework structure with the same sublattice topology,²⁰ but this structure differs from **III** in that only one linker, bis(4-

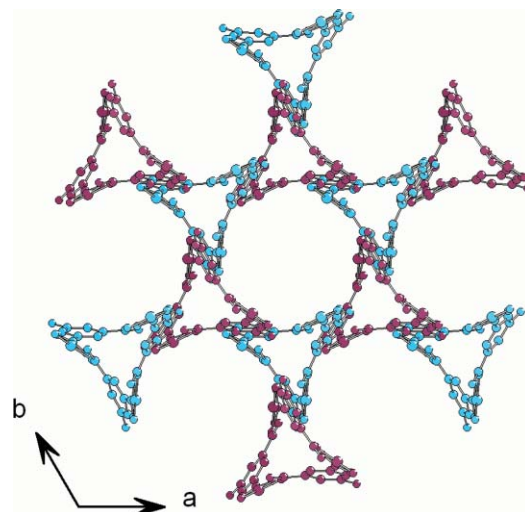


Fig. 10 A portion of the Kagome-like lattice in **III** formed by nickel–HIP helices propagating along c , with atoms color-coded by sublattice and hydrogen atoms omitted for clarity.

pyridyl)ethyne, provides all of the connections, and in that the sublattices differ slightly from each other.

A fivefold-interpenetrating zinc–bis(pyridyl)ethane–HIP in $P4_1$ was reported by Li *et al.*^{7b} In this compound, half of the 4_1 axes are encircled by atoms of only one sublattice, with sections of the other four merely cutting through, while the other half of the 4_1 axes are encircled by atoms contributed from four different sublattices. Thus, there is no superposition of screw axes to generate higher overall symmetry, as in **III**. Li *et al.* have also described interpenetrating but centrosymmetric coordination polymers of Co, Ni, and Cd with HIP and 1,3-bis(4-pyridyl)propane;²¹ the Ni compound exhibits Ni(II) in a coordination environment nearly identical to that seen in **III**. Hu and Tong reported the only other chiral hexagonal multiply-interpenetrating coordination polymer that we are aware of: a bis(pyridyl)propane-templated copper iodide in $P6_5/22$ consisting of three trigonally-symmetric sublattices.²² In this compound, the overall 6_6 symmetry arises from the collinearity of pairs of 3_2 axes from different sublattices, themselves related *via* perpendicular 2-fold axes. This differs slightly from **III** in that the combination of trigonal sublattices into a hexagonal structure occurs *via* other symmetry elements, whereas in **III** it occurs merely by the relative positioning of the sublattices.

Structure of **IV**, $\text{Cu}(\text{HIP})_2(\text{bipy})$

Compound **IV** (Fig. 11) crystallizes in the space group $C2/c$ and is a one-dimensional coordination polymer that also contains infinite hydrogen-bonded molecular ribbons (Fig. 12). It is also anhydrous, which is unusual for a coordination polymer obtained at 125 °C but common in those synthesized at significantly higher temperatures.²³ The chains consist of highly Jahn–Teller distorted *trans*- CuN_2O_4 octahedra connected linearly along b by bipy ligands, as in **I–III**. We suspect that it is primarily due to this distortion that no Cu(II) isomorphs to any of the other phases were ever produced, even under otherwise identical conditions. The four equatorial oxygens belong to two equivalent non-bridging HIP ligands, with the Cu1–O3 bond normal in length (1.965(2) Å) and the Cu1–O4 bond both elongated (2.685(3) Å) and bent

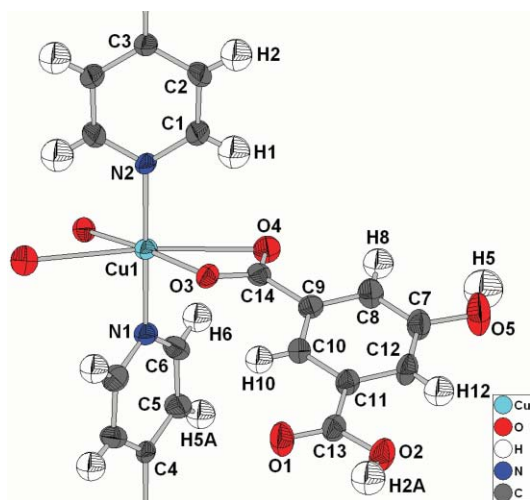


Fig. 11 Thermal ellipsoid plot (50% probability) of IV, with the atoms of one asymmetric unit labeled.

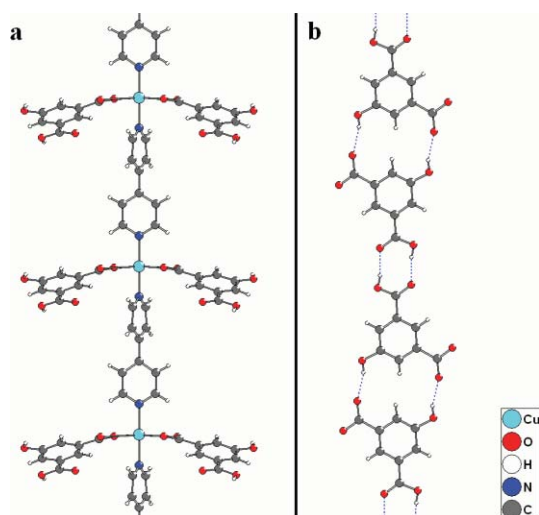


Fig. 12 (a) One copper–bipy chain with pendant HIP ligands, and (b) one doubly hydrogen-bonded ribbon of HIP ligands in IV, with hydrogen bonds dotted in dark blue.

approximately 35° out of perpendicularity to its neighbors. The HIP ligands are related by the two-fold rotation axis through the Cu–bipy chain and torqued oppositely about their C–C single bonds, which leaves them inclined approximately 30° in opposite directions out of the *ac* plane.

Infinite hydrogen-bonded arrays in IV are facilitated by the protonation of the non-coordinating carboxyl groups of the HIP ligands. Such HIP monoanions are much less common than HIP dianions, but are reported in a distorted Zr(II) complex in which the deprotonated carboxyl group coordinates asymmetrically through both oxygens,²⁴ and in a square-pyramidal Cu(II) complex in which only one oxygen coordinates.²⁵ Within the present family, protonation of carboxyl groups is unique to IV and allows each anion to participate in pairs of hydrogen bonds with symmetry-equivalent anions at either end, as seen in certain organic molecular crystals.²⁶ At one end, the anion donates a hydrogen bond from its phenol oxygen to a coordinating carboxyl oxygen of a neighboring anion, and accepts a second equivalent hydrogen

bond. This particular pairing of HIP groups, with hydrogen bonds exchanged between carboxyl and hydroxyl oxygens, is seen in Burchell and coworkers' 1,4-diazabicyclo[2.2.2]octane–5-hydroxyisophthalic acid complex,²⁷ in which the HIP groups are monoanionic as in IV. At the other end, the protonated carboxyl group exchanges two equivalent hydrogen bonds with the equivalent carboxyl group of another neighboring anion, in a typical carboxylic acid dimer arrangement. Thus, the HIP ligands are connected into linear ribbons by pairs of hydrogen bonds, and the ribbons run along two differently inclined directions related by the two-fold rotation axes in the Cu–bipy chains (Fig. 13). Because many different Cu–bipy chains contribute their HIP ligands to occupy each interchain space, the HIP ribbons stack tightly, with three per cell along the *b* direction and a ribbon-to-ribbon spacing of 3.40 Å. Thus, along the *c* axis, sheets of Cu–bipy chains alternate with sheets of stacked HIP ribbons, which themselves alternate in their direction of inclination (Fig. 14).

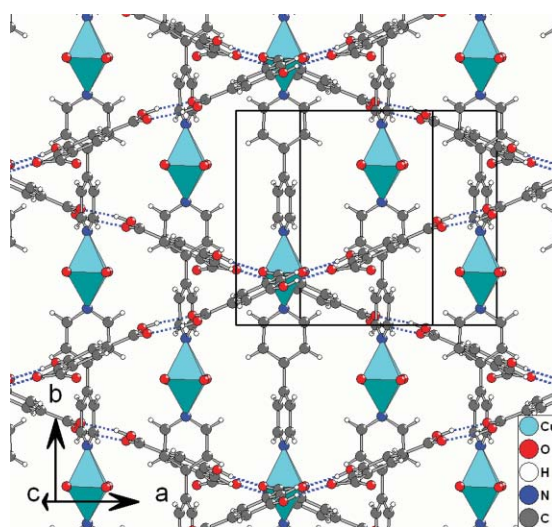


Fig. 13 A section of the structure of IV, viewed toward a layer of copper–bipy chains. Only every third HIP ribbon is shown for clarity, with hydrogen bonds dotted in dark blue.

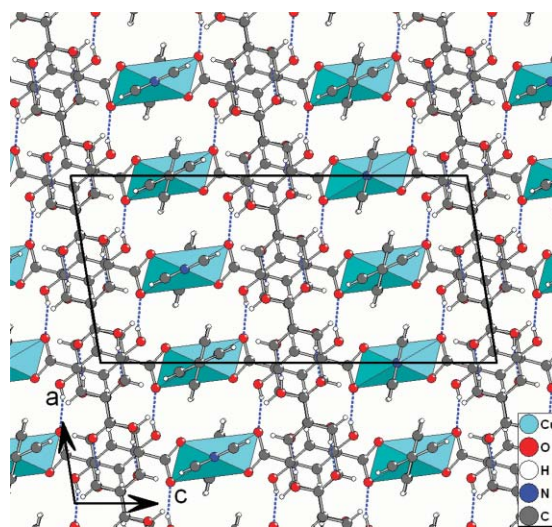


Fig. 14 Packing diagram of IV, viewed along the copper–bipy chains, approximately perpendicular to the HIP ribbons, with hydrogen bonds dotted in dark blue.

Structure of V, $\text{Zn}_2(\text{HIP})_2(\text{bipy})(\text{H}_2\text{O})_2 \cdot \text{H}_2\text{O}$

Compound V (Fig. 15) crystallizes in the space group $P\bar{1}$, and is a two-dimensional coordination polymer consisting of stair-stepped layers in (-111) planes. The zinc exhibits approximately trigonal bipyramidal coordination, with pairs of coordination polyhedra sharing edges around inversion centers to form dimers (Fig. 16). The distortion of the polyhedron is most suggestive of a capped tetrahedron; the Addison τ parameter²⁸ was calculated to be 0.703 indicating 29.7% square pyramidal character, when defining angle α as O5-Zn1-N1 and angle β as O6-Zn1-O3 . The three unshared ligand atoms are 1.920(2)–2.073(4) Å from Zn1, and O3 is shared, with a typical bond (1.962(3) Å) to one zinc atom and a long bond (2.741(3) Å) to its symmetry equivalent. Similar double bridging of $[4 + 1]$ -coordinated Zn(II) centers about an inversion center has been seen both in inorganic solids²⁹ as well as in molecular complexes,³⁰ however previous examples have not shown the degree of asymmetry seen in V. The $\text{Zn}_2\text{O}_6\text{N}_2$ dimers are connected along $[101]$ by single bipy ligands, and along $[110]$ by pairs of non-coplanar but parallel HIP ligands (Fig. 17). The HIP ligands lie parallel to the overall (-111) layers, and the bipy ligands nearly so. Stair-stepping in the layers arises because the bipy ligands connect the bottom members of a chain of $\text{Zn}_2\text{O}_6\text{N}_2$ dimers to the top members of the next chain. Between the bipy ligands lie water molecules which appear disordered across inversion centers, with two half-occupied components lying 2.16 Å away from each other (Fig. 18).

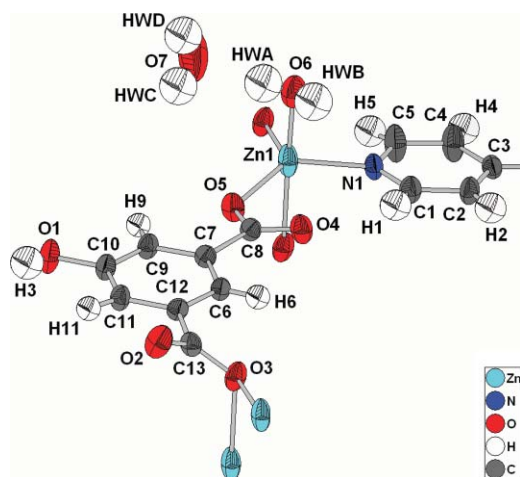


Fig. 15 Thermal ellipsoid plot (50% probability) of V, with the atoms of one asymmetric unit labeled. The occupancy of the uncoordinated water molecule is 1/2.

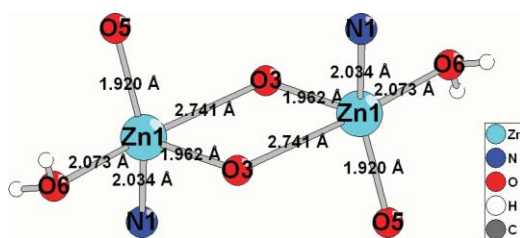


Fig. 16 One centrosymmetric $\text{Zn}_2\text{N}_2\text{O}_6$ dimer in V, showing the significant asymmetry of the bond lengths to the bridging oxygen O3.

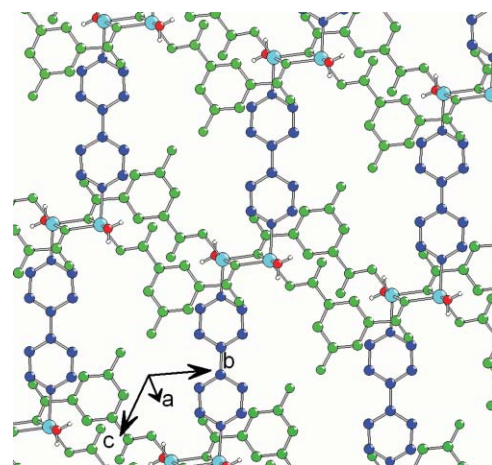


Fig. 17 Plan view of one layer in V, with HIP ligands in green, bipy ligands in dark blue, and zinc cations and water molecules colored as in Fig. 15 and 16. The HIP and bipy ligands connect zinc dimers along two nearly perpendicular directions. Ligand hydrogen atoms and uncoordinated water molecules are omitted for clarity.

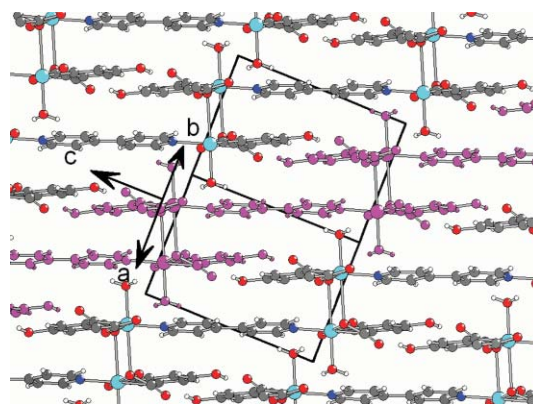


Fig. 18 Packing diagram of V, viewed from the side of the stair-stepped layers, with one layer highlighted in pink and other atoms colored as in Fig. 15 and 16.

Both carboxyl groups of each HIP ligand coordinate through only one oxygen, leaving the non-coordinating oxygen available to accept a hydrogen bond. This, in addition to a higher degree of hydration than III or IV, allows for the formation of rather extensive interlayer hydrogen bonding in V. Pairs of hydrogen bonds occur about inversion centers between approximately coplanar pairs of HIP ligands from consecutive layers, from the phenol hydrogens to one non-coordinating carboxyl oxygen, forming the same carboxyl/hydroxyl pairing arrangement as seen in IV. The aqua ligands supply additional interlayer hydrogen bonds to the other non-coordinating HIP carboxyl oxygen. Both equivalent disorder components of the uncoordinated water molecule accept hydrogen bonds from aqua ligands in one layer and donate hydrogen bonds to HIP phenol oxygens in the next layer.

Conclusion

By utilizing 5-hydroxyisophthalic acid together with 4,4'-bipyridyl to construct transition metal-based coordination polymers, we

have produced a wide and unexpected variety of new framework structures, including examples of one-, two- and three-dimensional covalent connectivity. The two Mn phases together provide the best example to date of polytypism in the field of coordination polymers. The Ni phase is an intricate interpenetrating 3D chiral network with unusual topology which, in projection, displays a classic Kagome lattice motif. The Cu phase is a rare example of a hybrid framework containing hydrogen-bonded molecular ribbons within its structure. Finally, the Zn phase is constructed from a unique infinite stair-stepped building unit. In all cases, the HIP ligand's phenolic oxygen remains protonated, but the ligand can be either singly or doubly deprotonated at its two carboxyl groups. In addition, this family of compounds has illustrated the sensitivity of the overall framework structures to fine nuances in the coordination geometry preferences of the metal cations that they contain.

Acknowledgements

The authors thank Guang Wu, Kinson Kam, James Orton and Crystal Merrill for valuable discussion. This work was supported by the U.S. Department of Energy, Office of Basic Energy Sciences, under Award Number DE-FG02-04ER46176.

References

- 1 B. F. Hoskins and R. Robson, *J. Am. Chem. Soc.*, 1990, **112**, 1546.
- 2 (a) A. K. Cheetham, C. N. R. Rao and R. K. Feller, *Chem. Commun.*, 2006, 4780; (b) C. N. R. Rao, S. Natarajan and R. Vaidyanathan, *Angew. Chem., Int. Ed.*, 2004, **43**, 1466; (c) M. O'Keeffe, M. Eddaoudi, H. Li, T. Reineke and O. M. Yaghi, *J. Solid State Chem.*, 2000, **152**, 3.
- 3 Q. Shuai, S. Chen and S. Gao, *Inorg. Chim. Acta*, 2007, **360**, 1381.
- 4 (a) X.-H. Sun, *Acta Crystallogr., Sect. E*, 2005, **61**, m2256; (b) H.-P. Xiao, *Acta Crystallogr., Sect. E*, 2006, **62**, m731; (c) Z.-W. Wang, Y.-Z. Li, Y. Cai and H.-G. Zheng, *Acta Crystallogr., Sect. E*, 2006, **62**, m734; (d) M. J. Plater, M. R. St. J. Foreman, R. A. Howie, J. M. S. Skakle, S. A. McWilliam, E. Coronado and C. J. Gómez-García, *Polyhedron*, 2001, **20**, 2293.
- 5 H. Xu and Y. Li, *J. Mol. Struct.*, 2004, **690**, 137.
- 6 (a) J. M. S. Skakle, M. R. St. J. Foreman and M. J. Plater, *Acta Crystallogr., Sect. E*, 2001, **57**, m373; (b) X.-Y. Cao, J. Zhang, Y. Kang, J.-K. Cheng, Z.-J. Li, X.-Q. Wang and Y.-G. Yao, *Acta Crystallogr., Sect. E*, 2004, **60**, m460; (c) X.-Y. Cao, J. Zhang, Y. Kang, J.-K. Cheng, Z.-J. Li, X.-Q. Wang, Y.-H. Wen and Y.-G. Yao, *Acta Crystallogr., Sect. C*, 2004, **60**, m350.
- 7 (a) H.-Y. He, Y.-L. Zhou, Y. Hong and L.-G. Zhu, *J. Mol. Struct.*, 2005, **737**, 97; (b) X. Li, R. Cao, D. Sun, W. Bi, Y. Wang, X. Li and M. Hong, *Cryst. Growth Des.*, 2004, **4**(4), 775.
- 8 G. M. Sheldrick, *SHELXTL-97, A Program for Crystal Structure Solution and Refinement*, University of Göttingen, Göttingen, Germany, 1997 (Ver. 5.1).
- 9 A. L. Spek, *PLATON—A Multipurpose Crystallographic Tool*, Utrecht University, Utrecht, The Netherlands, 2005.
- 10 G. M. Sheldrick, *SADABS User Guide*, University of Göttingen, Göttingen, Germany, 1995.
- 11 H. D. Flack, *Acta Crystallogr., Sect. A*, 1983, **39**, 876–881.
- 12 (a) C. Ma, C. Chen, Q. Liu, D. Liao, L. Li and L. Sun, *New J. Chem.*, 2003, **27**, 890; (b) J. Tao, X.-M. Chen, R.-B. Huang and L.-S. Zheng, *J. Solid State Chem.*, 2003, **170**, 130.
- 13 (a) D. L. Smith and V. I. Saunders, *Acta Crystallogr., Sect. B*, 1981, **37**, 1807; (b) D. L. Smith and V. I. Saunders, *Acta Crystallogr., Sect. B*, 1982, **38**, 907.
- 14 R. D. Willett, K. R. Maxcy and B. Twamley, *Inorg. Chem.*, 2002, **41**, 7024.
- 15 A. Guinier, G. B. Bokij, K. Boll-Dornberger, J. M. Cowley, S. Đurovič, H. Jagodzinski, P. Krishna, P. M. De Wolff, B. B. Zvyagin, D. E. Cox, P. Goodman, T. Hahn, K. Kuchitsu and S. C. Abrahams, *Acta Crystallogr., Sect. A*, 1984, **40**, 399.
- 16 J. A. Groves, P. A. Wright and P. Lightfoot, *Inorg. Chem.*, 2005, **44**, 1736.
- 17 (a) M. Kurmoo, H. Kumagai, M. Akita-Tanaka, K. Inoue and S. Takagi, *Inorg. Chem.*, 2006, **45**, 1627; (b) J. Chen, M. Ohba, D. Zhao, W. Kaneko and S. Kitagawa, *Cryst. Growth Des.*, 2006, **6**(3), 664.
- 18 Y.-Q. Zheng and Z.-P. Kong, *Z. Anorg. Allg. Chem.*, 2003, **629**, 1469.
- 19 (a) V. A. Blatov, *IUCr Commission on Crystallographic Computing Newsletter*, (no. 7), Nov. 2006, p. 4 (URL: <http://www.iucr.org/iucr-top/comm/ccom/newsletters/>); (b) <http://topos.ssu.samara.ru/>.
- 20 L. Carlucci, G. Cianì, P. Macchi and D. M. Proserpio, *Chem. Commun.*, 1998, 1837.
- 21 X.-J. Li, R. Cao, W.-H. Bi, Y.-Q. Wang, Y.-L. Wang and X. Li, *Polyhedron*, 2005, **24**, 2955.
- 22 S. Hu and M.-L. Tong, *Dalton Trans.*, 2005, 1165.
- 23 P. M. Forster, A. R. Burbank, C. Livage, G. Férey and A. K. Cheetham, *Chem. Commun.*, 2004, 368.
- 24 Y.-J. Zhao, R.-W. Liu and X.-H. Li, *Acta Crystallogr., Sect. E*, 2005, **61**, m535.
- 25 H.-P. Xiao, W.-D. Wang, W.-B. Zhang and J.-G. Wang, *Acta Crystallogr., Sect. E*, 2005, **61**, m841.
- 26 M. C. Grossel, C. A. Golden, J. R. Gomm, P. N. Horton, D. A. S. Merkel, M. E. Oszer and R. A. Parker, *CrystEngComm*, 2001, **3**, 170.
- 27 C. J. Burchell, G. Ferguson, A. J. Lough and C. Glidewell, *Acta Crystallogr., Sect. C*, 2000, **56**, 1126.
- 28 A. W. Addison, T. N. Rao, J. Reedijk, J. van Rijn and G. C. Verschoor, *J. Chem. Soc., Dalton Trans.*, 1984, 1349.
- 29 R. J. B. Jakeman and A. K. Cheetham, *J. Am. Chem. Soc.*, 1988, **110**(4), 1142.
- 30 M. Barceló-Oliver, A. Terrón, A. García-Raso, J. J. Fiol, E. Molins and C. Miravittles, *J. Inorg. Biochem.*, 2004, **98**, 1703.